Annealing Textures of Heavily Rolled 50%Ni-Fe Thin Sheets*

Haruo KATO

The Research Institute for Iron, Steel and Other Metals

(Received August 20, 1971)

Synopsis

The present investigation was undertaken to study the annealing textures of 50%Ni-Fe alloy specimens which were heavily rolled to a very much reduced thickness and the recrystallization mechanisms of (100)[001] texture component are discussed.

(1) It has been recognized that the rolling textures of this alloy indicate the copper-type up to this time, but it is unable to simply describe as the copper-type texture since it shows a peculiar texture under such an extreme rolling condition.

(2) Very weak (100)[001] texture component still remains in a deformed matrix but this component decreases still more, after a heavy reduction higher than 99.4% or in a thinner sheet than 20 μ.

(3) The number of nuclei of (001)[100] recrystallization texture component has a mutual relationship with the intensity of (001)[100] texture component in a deformed matrix.

(4) Cube component decreases remarkably and the components similar to rolling textures increase gradually in proportion to the reduction of thickness after annealing.

(5) It is considered that the preformed nucleation model, proposed by Beck and Cahn is appropriate to account for the recrystallization mechanism, but it would be rather more rigorous to express it as "the orientated nucleation and interacted growth theory".

I. Introduction

Many investigators have reported with regard to the recrystallization mechanism up to this time and the current theories on the nucleation theory in recrystallization of single phase in metals and alloys have been summarized by R.W. Cahn[1] as follows:

All of these theories are developed on the bases either of the classical nucleation model,[2]~[6] the martensitic nucleation model,[7],[8] the preformed nucleation

* The **1526th** report of the Research Institute for Iron, Steel and Other Metals. Presented at the General Meeting of the Japan Institute of Metals, in Tokyo, in March, 1969.

(1) ASM, *Recrystallization, Grain Growth and Textures*, Chapman and Hall, (1966), 99.
(2) R. Becker, Z. Tech. Physik, **7** (1926), 547.
(3) E. Orowan, *Dislocation in Metals*, AIME (1954), 181.
(4) J.E. Burke and D. Turnbull, Prog. Met. Phys., **3** (1952), 220.
(5) R.A. Oriani, Acta Met., **8** (1960), 134.
(6) J.E. Bailey, Phil. Mag., **5** (1960), 833.
(7) C.A. Verbraak, Acta Met., **6** (1958), 580.
(8) W.G. Burgers and C.A. Verbraak, Acta Met., **5** (1957), 765.

model[8]~[15] or the Bulge nucleation model.[5]

In the previous paper[16] we have investigated the cold rolling textures of heavily rolled and ultra-thin sheets in 50%Ni-Fe alloy. It has been recognized that the rolling textures of this alloy indicate peculiar textures under such extreme rolling conditions, i.e. — (1) The center textures up to 99.4% reduction and in the sheets thicker than 20 μ show the sharp copper-type, (2) After much higher reduction than 99.4% the {110}⟨112⟩ texture component decreases and the {112}⟨111⟩ texture component increases and such tendency is more remarkable in the thinner sheets and in the surface layer, (3) After much higher reduction than 99.9%, weak {110}⟨335⟩ and the {110}⟨100⟩ texture component increase little by little with increase of reduction and is stronger in the surface layer, (4) Very weak {100}⟨001⟩ texture component remains in the deformed matrix while after heavy reduction more than 99.4% and in the sheets thinner than 20 μ, this component decreases still more, and also the intensity in the recrystallized cube texture decreased remarkably. It is considered that the cause of this inferiority in a cube texture has not been elucidated clearly up to this time.

The present investigation was undertaken to study the annealing textures of specimens of the ultra-thin thickness due to ultra-high reduction in 50%Ni-Fe alloy, and the recrystallization mechanism of the (100)[001] texture component were discussed.

II. Experimental method and specimens

The 50%Ni-Fe alloy used in the experiment was fabricated by melting by a high frequency induction furnace under high vacuum. The 50 kg ingots consist of 0.02% C, 0.002% P, 0.24% Mn, 0.40% Co, 50.82% Ni and residual Fe were forged, hot rolled and then cold rolled to strips of 0.15~0.006 mm in thickness, as shown in Table 1. As in Table 1, each intermediate annealing during cold rolling processes was done at 850°C for 3 hr in hydrogen, the grain size of the plates just before finishing rolling were 0.03~0.06 mm in diameter.

The sheets were reversely rolled down to 3 mm with a 2-Hi mill, then rolled to 0.15 mm with a 4-Hi mill and the thickness less than 0.15 mm were attained with a 20-Hi mill, those which having 300, 150 and 6 mm dia. roll respectively. The draught per pass was about 10% and the total reductions of specimens were reached from 86.5 to 99.97%. Mainly, three specimens among them are used in

(9) K. Detert and J. Ziebs, Trans. AIME, **233** (1965), 51.
(10) P.A. Beck, J. Appl. Phys., **20** (1949), 633.
(11) R.W. Cahn, Proc. Phys. Soc., London, **63A** (1950), 323.
(12) J.E. Bailey and P.B. Hirsch, Proc. Roy. Soc., **267A** (1962), 11.
(13) H. Hu, *Recovery and Recrystallization of Metals*, Interscience, New York (1963), 311.
(14) J.L. Walter and G.F. Koch, Acta Met., **11** (1963), 923.
(15) J.C.M. Li, J. Appl. Phys., **33** (1962), 2958.
(16) H. Kato and E. Tanaka, J. Japan Inst. Metals, **33** (1969), 385 (in Japanese); Sci. Rep. RITU, **A 20** (1969), 177.

Table 1. Rolling schedule of specimens.

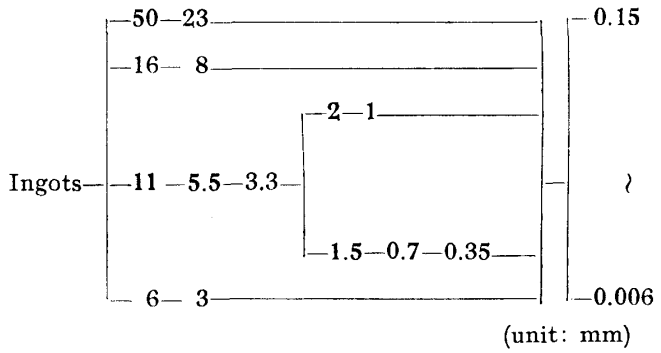

the experiment, namely, those of 50 μ (99.4% red.), 12 μ (99.85% red.) and 7 μ (99.91% red.) in thickness. Annealing after cold rolling was done in vacuum furnace ($<5\times10^{-4}$ mmHg), by operating which the specimens held in cooling chamber are inserted in a heating zone, held for 1/2 hr at each temperature and again pulled out in water cooled stainless steel chamber.

The development of annealing textures was studied by examining complete pole figures determined from the (111) and (200) reflection using Co-K_α radiation by means of Decker-Harker's method.

Details of light and electromicroscopic observation of recrystallization progress shall be reported in the sequential papers.[17]

III. Results

1. Rolling texture

Typical (111) and (200) pole figures in middle layers of sheets rolled as thin as 50, 12 and 7 μ in thickness, corresponding to the reductions of 99.4%, 99.8 and 99.91% respectively, are shown in Figs. 1~3. The pole figures of middle layer seem to represent a typical copper-type texture but when the thickness becomes from 50 to 7 μ, the so-called sharp copper-type texture begins to change, the sharp (110)[$\bar{1}$12] orientation rotates to the (112)[$\bar{1}$11] and (110)[$\bar{3}$35] orientations. These details and the thickness effect on texture transition observed in the specimens subjected to an ultra-high reduction and also in an ultra-thin thickness was reported already.[16]

Fig. 4 shows the variation of intensity distribution along the peripheral circle of (200) diffraction line observed in the specimen rolled 99.4% and 50 μ in thickness and that rolled 99.91% and 7 μ in thickness. In the former cases a very sharp (110)[$\bar{1}$12] texture component and a weak cube component are observable while in the latter case a sharp (110)[$\bar{3}$35] texture component and a very weak cube component are seen. And the former has very sharp cube component and the

(17) Presented at the General Meeting of the Japan Institute of Metals, in Amagasaki, in October, 1970 and in Tokyo, in April,

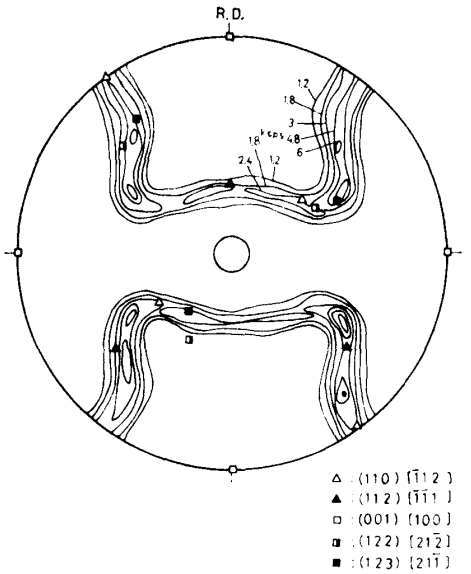

Fig. 1 (a)

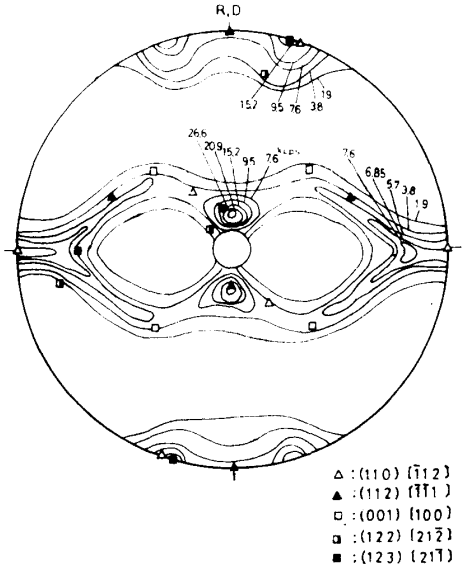

Fig. (b)

Fig. 1-a. (200) pole figure for the rolling texture of the sheet, 50 μ thick, rolled 99.4%.
Fig. 1-b. (111) pole figure for the rolling texture of the sheet, 50 μ thick, rolled 99.4%.

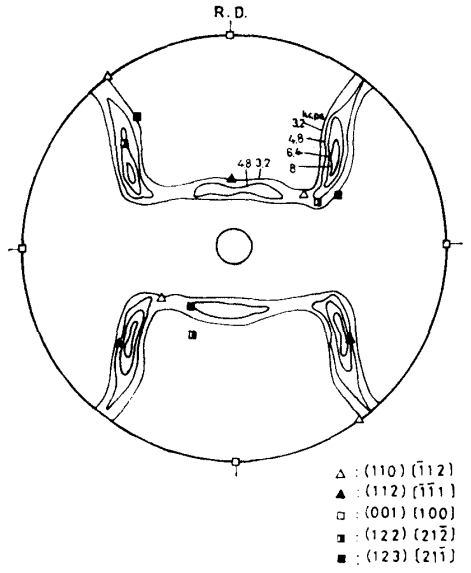

Fig. 2 (a)

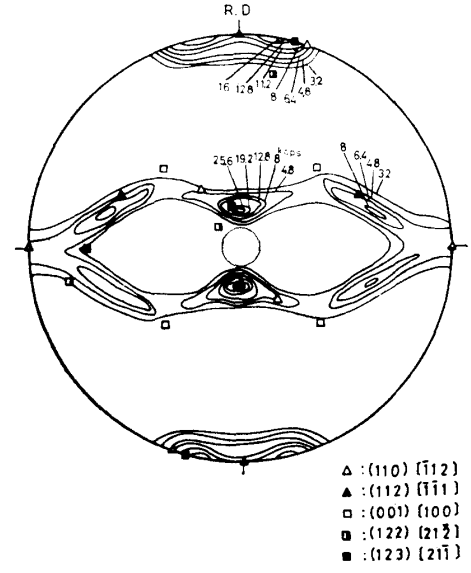

Fig. 2 (b)

Fig. 2-a. (200) pole figure for the rolling texture of the sheet, 12 μ thick, rolled 99.8%.
Fig. 2-b. (111) pole figure for the rolling texture of the sheet, 12 μ thick, rolled 99.8%.

latter has a weak cube component after recrystallization. The (110)[$\bar{1}$12] texture component rotates to the (112)[$\bar{1}$11] and the (110)[$\bar{3}$35] texture components, it appears that the final thickness has a larger effect on the orientation rotation than the rate of reduction.[16]

2. Annealing textures

Figs. 5 and 6 show the variation of integrated intensities of cube component

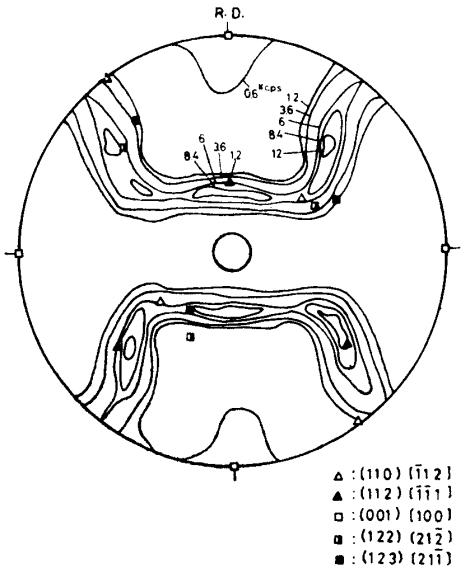

Fig. 3 (a)

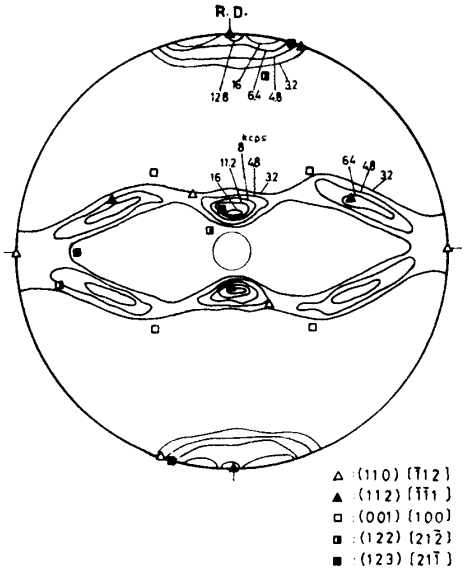

Fig. 3 (b)

Fig. 3-a. (200) pole figure for the rolling texture of the sheet, 7 μ thick, rolled 99.9%
Fig. 3-b. (111) pole figure for the rolling texture of the sheet, 7 μ thick, rolled 99.9%.

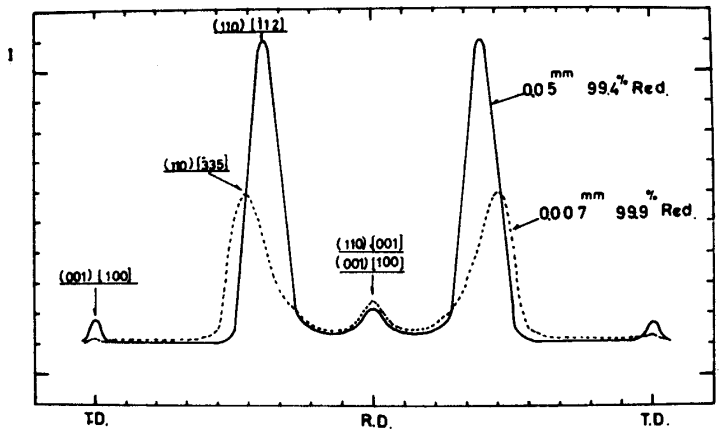

Fig. 4. Variation of intensity distribution along the circle ($\alpha=0°$) in (200) pole fig.

at the transverse direction along the peripheral circle of diffraction lines on annealing. The (001)[100] texture component in the partially recrystallized deformed matrix diminishes remarkably when the thickness is much decreased, particularly, in case the thickness becomes less than 10 μ, and the reduction amounts to more than 99.4%. It is clear from this figures that the number (or intensity) of (001)[100] recrystallized nuclei are mutually related to the intensity (001)[100] texture component in a deformed matrix. The intensity of recrystallized cube component correspond to the intensity of cube component remained in a deformed matrix.

Figs. 7~11 show the annealing textures of each specimen annealed at 540°C for 1/2 hr.

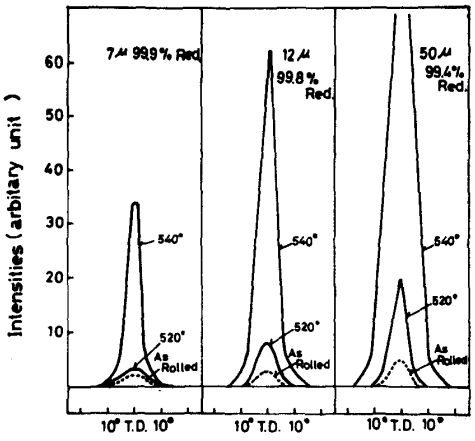

Fig. 5

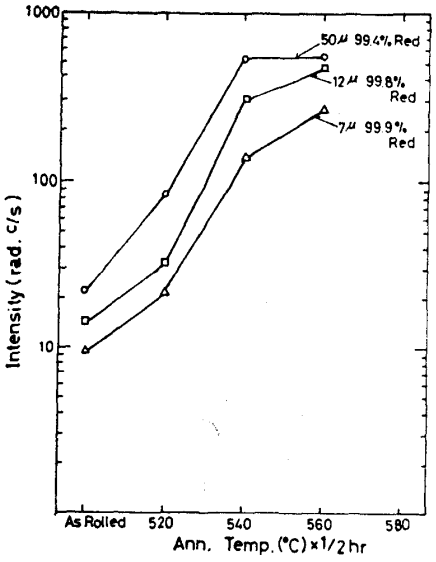

Fig. 7

Fig. 5. Variation of integrated intensities along the peripheral circle of (200) diffraction lines on annealing.

Fig. 6. Variations of integrated intensities along the peripheral circle of (200) diffraction lines on annealing.

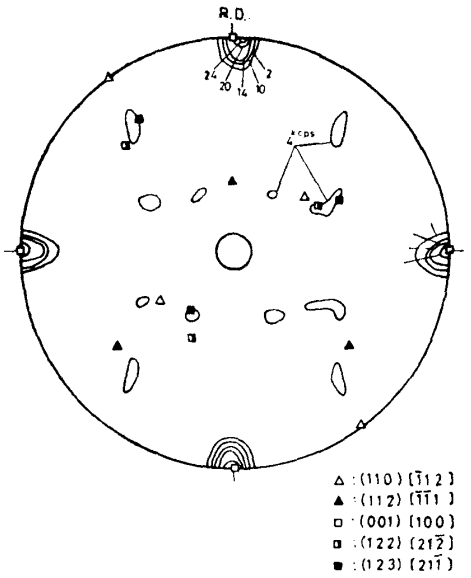

Fig. 7

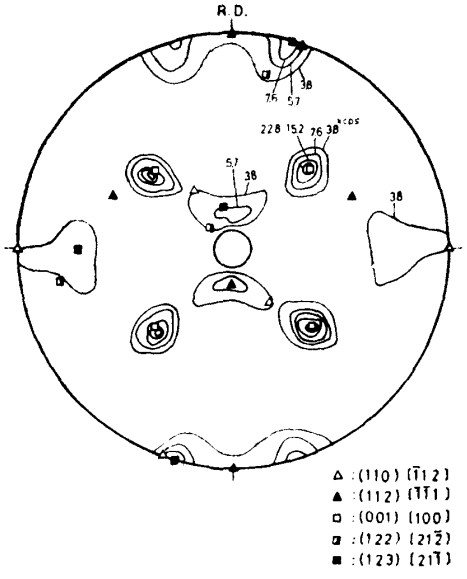

Fig. 9

Fig. 7. (200) pole figure for the annealed texture of the sheet, 50 μ thick, rolled 99.4% and annealed at 540°C for 1/2 hr.

Fig. 8. (111) pole figure for the annealed texture of the sheet, 50 μ thick, rolled 99.4% and annealed at 540°C for 1/2 hr.

The sheet, 50 μ in thickness recrystallized about 70% in area, consisting of the sharp cube texture, the weak twin component and residual being (110)[$\bar{1}$12], (112)[$\bar{1}$11] and (123)[21$\bar{1}$] rolling textures. The annealing textures of 12 and 7 μ in thickness that the progress of recrystallization are delayed conspicuously are

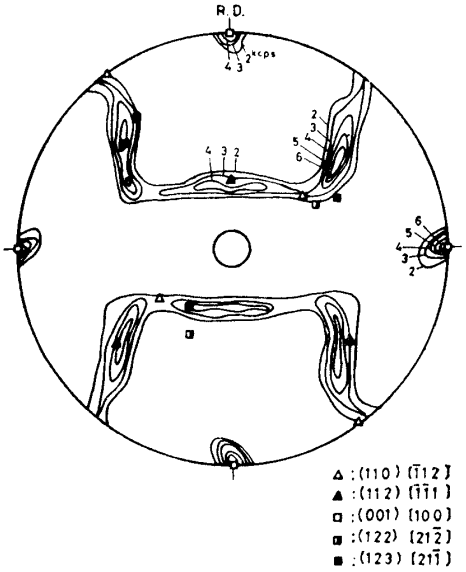

Fig. 9

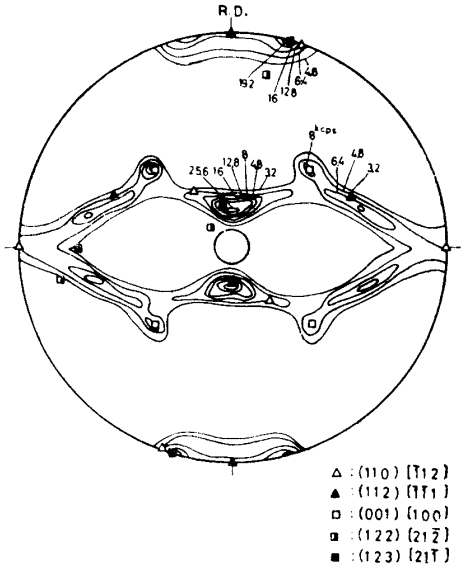

Fig. 10

Fig. 9. (200) pole figure for the annealed texture of the sheet, 12 μ thick, rolled 99.8% and annealed at 540°C for 1/2 hr.

Fig. 10. (111) pole figure for the annealed texture of the sheet, 12 μ thick, rolled 99.8% and annealed at 540°C for 1/2 hr.

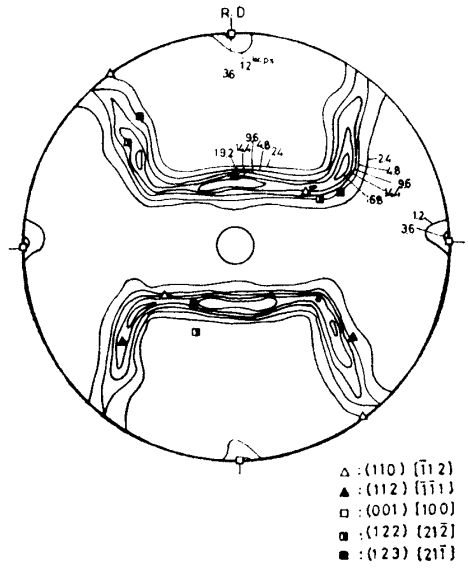

Fig. 11

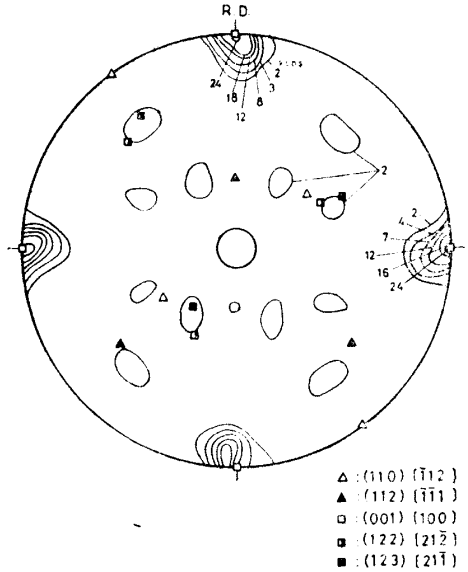

Fig. 12

Fig. 11. (200) pole figure for the annealed texture of the sheet, 7 μ thick, rolled 99.9% and annealed at 540°C for 1/2 hr.

Fig. 12. (200) pole figure for the annealed texture of the sheet, 50 μ thick, rolled 99.4% and annealed at 580°C for 1/2 hr.

component of the rolling texture mainly and the weak cube texture, very weak twin of cube texture and the other component being similar rolling texture, for example, the (123)[21$\bar{1}$] texture component.

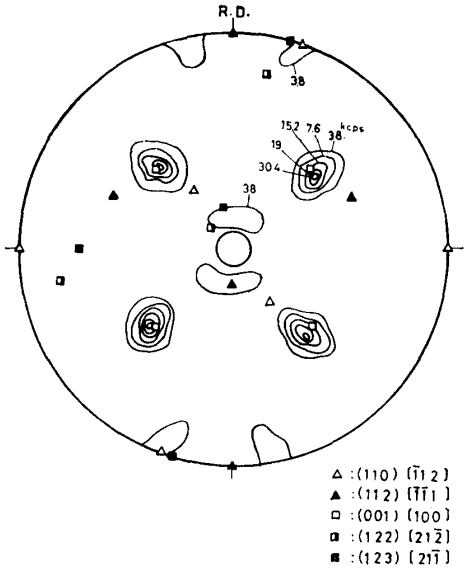

Fig. 13

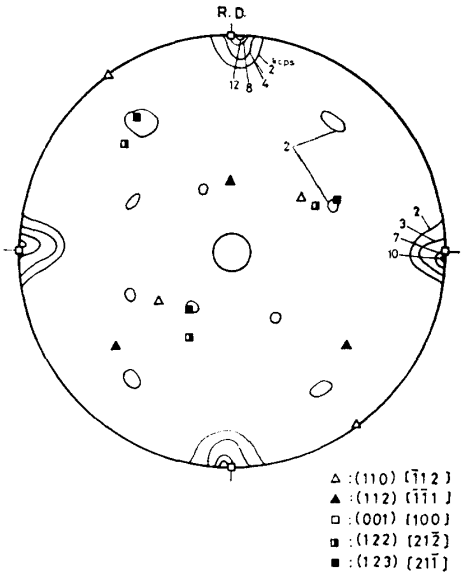

Fig. 14

Fig. 13. (111) pole figure for the anneald texture of the sheet, 50 μ thick, rolled 99.4% and annealed at 580°C for 1/2 hr.

Fig. 14. (200) pole figure for the annealed texture of the sheet, 12 μ thick, rolled 99.8% and annealed at 580°C for 1/2 hr.

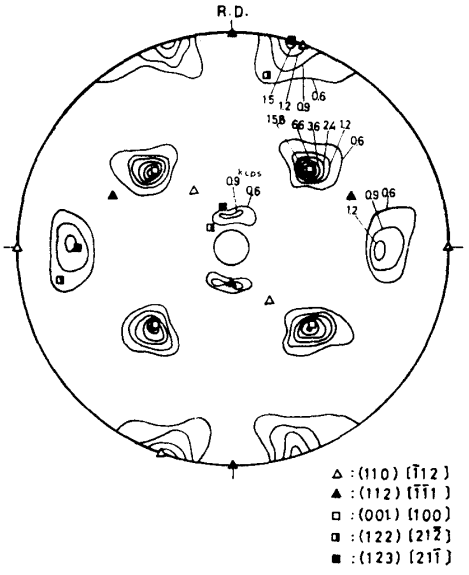

Fig. 15

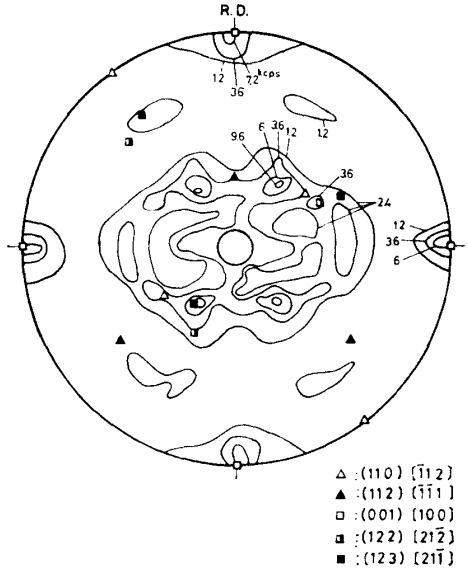

Fig. 16

Fig. 15. (111) pole figure for the annealed texture of the sheet, 12 μ thick, rolled 99.8% and annealed at 580°C for 1/2 hr.

Fig. 16. (200) pole figure for the annealed texture of the sheet, 7 μ thick, rolled 99.9% and annealed at 600°C for 1 hr.

The completely recrystallized textures at primary recrystallization are shown in Figs. 12~17. Textures of the sheet 50 μ thick are composed of very sharp cube texture, weak twin component of cube texture and the (123)[21$\bar{1}$] texture

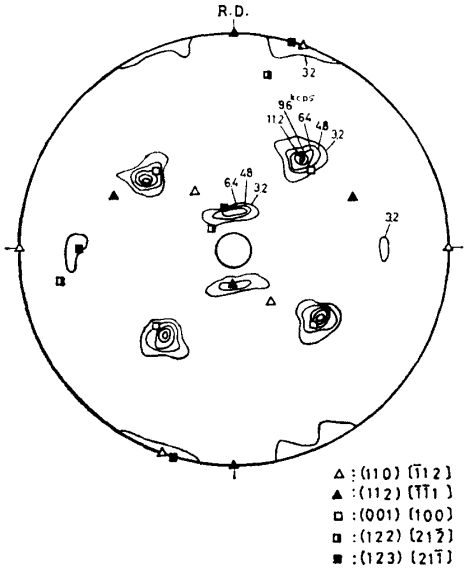

Fig. 17

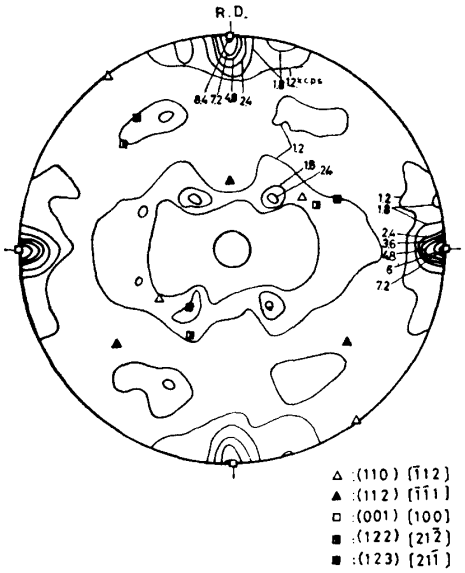

Fig. 18

Fig. 17. (111) pole figure for the annealed texture of the sheet, 7 μ thick, rolled 99.9% and annealed at 600°C for 1 hr.

Fig. 18. (200) pole figure for the annealed texture of the sheet, 7 μ thick, rolled 99.9% and annealed at 1000°C for 2 hr.

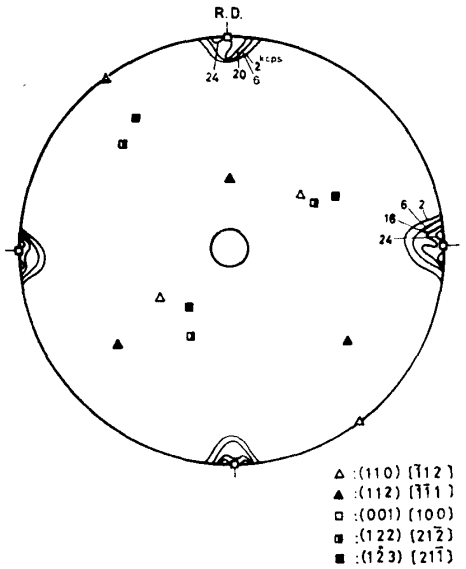

Fig. 19. (200) pole figure for the annealed texture of the sheet, 50 μ thick, rolled 99.4% and annealed at 1000°C for 2 hr.

component, but in accordance with the decrease in thickness cube component diminished remarkably and the components similar to rolling textures increased gradually; in consequence, the pole figures of 7 μ sheet differ from that of 50 μ sheet. These facts are obvious from the observation of (200) pole figure in 50 and 7 μ thick sheets, annealed at 1000°C for 2 hrs, as shown in Figs. 18 and 19.

IV. Discussion of results

The existence of (001)[100] cube component, as a minor component in the deformed matrix, rolled Fe-Ni alloy has been published in several reports already.[18]~[20]

It is very interesting that the intensity of (001)[100] recrystallization texture component are mutually related to the intensity of (001)[100] texture component in the deformed matrix. The fact that the remarkable decrement of the number of nuclei of (001)[100] recrystallization texture component in spite of the increment of twin related (112)[$\bar{1}$11] rolling texture in the ultra-thin and heavily rolled sheets, are considered to be discordant with the inverse-Rowland mechanism.[21]

The existence of (001)[100] texture component in the deformed matrix has been denied from the results by F. Haessner et al.[22] and K. Lücke et al.[23]

These results evince that no cube cell is observed in the rolled copper sheets by means of a selected area diffraction of the electron microscope. Total number of points detected are 600 in the former paper[22] and 234 in the latter.[23] But it would be premature to conclude so only from these results because the numbers detected are yet very few.

The existence fraction of the cube component in the deformed matrix are $1/10^4 \sim 1/10^3$ in 50%Ni-Fe alloy at rough estimate from our data[17] by means of the selected area diffraction of the electron microscope, the X-ray diffraction analysis and the optical microscopic observation.

Considering the recrystallization mechanism of cube texture, the pre-existing cube component, whose lattice is highly curved, release its highly stored energy at the earliest stage; i.e. in the recovery stage, the above-mentioned component becomes the low stored energy and would grow into the high stored surrounding matrix in the recrystallization stage.

Fig. 20 is the schematic diagrams[24] of the deformed process of artificially recrystallized cube grains. Cube grains rotate gradually to the rolling textures surrounding then and its elongated cube grains are eaten away parpendicular to the rolling direction. At the 95% reduction only the small area of cube grains are dotted in the deformed matrix, and the lattice of these dotted area is highly curved, that is, highly stored energy state.

The ordinate in Fig. 20-c shows the micro-Vicker's hardness; the values in deformed matrix are $322 \sim 339$ which have deformed matrix rotated from cube grains; 322 and remained cube area; 363, viz. the cube area has the highest hardness.

(18) G. Sachs and J. Sprentnak, Met. Tech., 1940, T.P., 1143.
(19) H. Abe and H. Seki, J. Japan Inst. Met., **23** (1959), 343.
(20) H. Nakae and A. Okada, J. Japan Inst. Met., **32** (1968), 375.
(21) C.A. Verbraak, Acta Met., **5** (1957), 765.
(22) F. Hasessner, U. Jakubonniski and M. Wilkens, Phys. Stat. Sol., **7** (1964), 701.
(23) L. Lücke, H. Perlwitz and W. Pitsch, Phys. Stat. Sol., **7** (1964), 733.
(24) H. Kato, to be published.

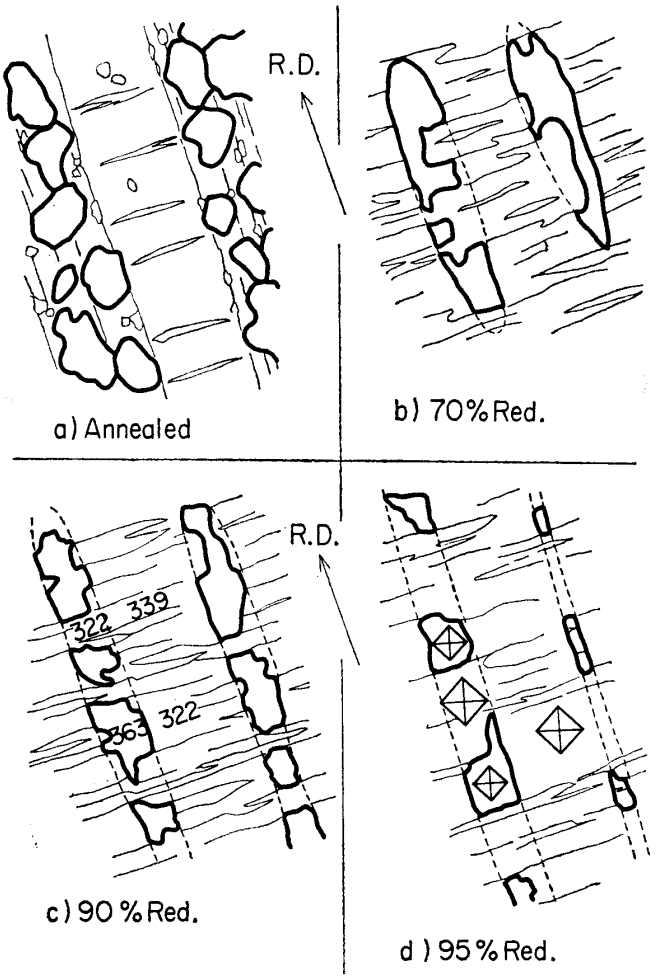

Fig. 20. Schematic diagrams in deformed process of (100) recryst. nuclei.

Moreover, according to the electron microscopic analysis[17] the cell size of remained cube are very larger than the cell of deformed matrix and its dislocation density is very high. The experimental results of microscopic direct observation on sub-grain growth with the electron microscope and the optical microscope will be published in a subsequent paper.[24]

Complying with Cahn's classification as mentioned above, it may be appropriate to accept the preformed nucleation model, but considering the next growth stage, it would be rather preferable to express it in terms of "an orientated nucleation and interacted growth theory".

Acknowledgements

The author wishes to express hearty thanks to Professor Dr. E. Tanaka for his helpful discussion throughout the study, Miss Y. Konno for her assistance in the X-ray analysis and members of laboratory for metalworking who rolled the specimens.